Investigation of GaN-based dual-wavelength light-emitting diodes with p-type barriers and vertically stacked quantum wells

Jun Chen (陈 峻)[1,2], Guanghan Fan (范广涵)[1*], Wei Pang (庞 玮)[2], Shuwen Zheng (郑树文)[1], and Yunyan Zhang (张运炎)[3]

[1]*Institute of Opto-Electronic Materials and Technology, South China Normal University, Guangzhou 510631, China*

[2]*Experimental Teaching Center, Guangdong University of Technology, Guangzhou 510006, China*

[3]*Department of Electronic and Computer Engineering, Hong Kong University of Science and Technology, Hong Kong, China*

[*]*Corresponding author: gfan@scnu.edu.cn*

Received September 22, 2011; accepted January 5, 2012; posted online March 15, 2012

Designs of p-doped in quantum well (QW) barriers and specific number of vertically stacked QWs are proposed to improve the optical performance of GaN-based dual-wavelength light-emitting diodes (LEDs). Emission spectra, carrier concentration, electron current density, and internal quantum efficiency (IQE) are studied numerically. Simulation results show that the efficiency droop and the spectrum intensity at the large current injection are improved markedly by using the proposed design. Compared with the conventional LEDs, the uniform spectrum intensity of dual-wavelength luminescence is realized when a specific number of vertically stacked QWs is adopted. Suppression of electron leakage current and the promotion of hole injection efficiency could be one of the main reasons for these improvements.

OCIS codes: 230.3670, 260.5430, 300.6170.

doi: 10.3788/COL201210.062302.

In recent years, following the remarkable improvement of the material growth and device fabrication technology, high-efficiency, and high-power white light-emitting diodes (LEDs) have made the outdoor full color display become feasible[1]. For luminescence, these conventional LEDs need phosphor to activate. In addition, such LEDs have short lifetime and low brightness because of the degradation of phosphor. In current structure, a novel structure of dual-wavelength LEDs has received extensive investigation. In this structure, two vertically stacked quantum wells (QWs) with different emitted colors are grown sequentially[2−5]. By adjusting the current injection or driving voltage of the LEDs, the luminescence for white or other colors can be realized. The advantages of this structure include phosphor-free and better optical performance compared with conventional LEDs. However, similar to the conventional nitride-based LEDs, troublesome issues such as severe efficiency droop[6,7] and the non-uniform spectrum intensity[8] are also present in these dual-wavelength LEDs. Severe electron leakage current may play an important role in the efficiency droop problem[9], and the thermionic carrier escape process in the active region could lead to poor current injection efficiency, as well as non-uniform distribution of carriers[10−13]. Various suggestions have been proposed to settle these issues and enhance the optical performance of the LEDs, such as adopting the staggered QWs or delta-QWs to obtain large electron-hole wavefunction overlap and spontaneous emission rate[14−18], improving the conventional AlGaN electron blocking layer (EBL) with the lattice-matched InAlN layer[19], utilizing the gradually increased AlGaN layer as EBL[20], altering GaN QW barrier with AlGaN[21], InGaN[22], or InAlGaN material[23], adopting InGaN QW barrier with gradually increased thickness[24], among others.

In this letter, with the purpose of improving the efficiency droop and the optical performance of the GaN-based dual-wavelength LEDs, the design of p-doped QW barriers is investigated numerically in detail. The hole injection efficiency is expected to be enhanced, and the electron spill over from the p-side could be hindered by the higher barrier due to the p-doped QW barriers. Moreover, a better balance for carrier distribution in each QW could be realized by adjusting the number of vertically stacked QWs.

The conventional dual-wavelength LEDs (structure A) are grown on a *c*-plane sapphire substrate with metal–organic chemical vapor deposition (MOCVD) as reference, followed by a 50-nm undoped GaN layer, and a 4.5-μm n-GaN layer (n-doping=5×10^{18} cm^{-3}). The active region consists of two vertically stacked active layers (I and II). On the n-side, each active layer has two-pair undoped QWs with two 2.2-nm InGaN wells and two 15-nm GaN barriers. The active layer I comprises $In_{0.11}Ga_{0.89}N$ QWs, whereas the active layer II comprises $In_{0.18}Ga_{0.82}N$ QWs. On top of the active region is a 30-nm p-$Al_{0.07}Ga_{0.93}N$ EBL and a 0.15-μm p-GaN cap layer (p-doping=7×10^{17} cm^{-3}). The device geometry is designed with a rectangular shape of 300×300 (μm). The schematics of the conventional LEDs are shown in Fig. 1. In order to improve the severe efficiency droop and enhance the optical performance, two other specifically designed epitaxial structures (B and C) are investigated. Structure B is the same as conventional LEDs, except that the undoped GaN barriers are replaced by p-doped barriers. Note that, in order to avoid the low electron injection into the last few QWs (near the p-side) and p-dopant diffusion into the QWs due to the heavy doping, gradually increased p-doped barriers are adopted (p-doping=$1\times10^{17}-7\times10^{17}$ cm^{-3}) in structure B. In conventional LEDs, a greater number of QWs will

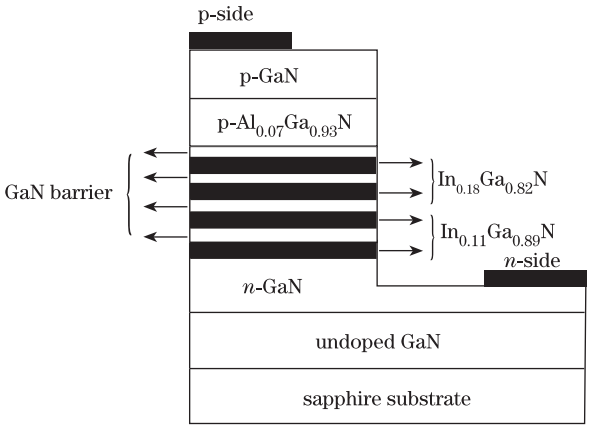

Fig. 1. Schematics of conventional LEDs.

deteriorate the LED performance[25]; however, for the vertically stacked QWs with p-doped barriers, higher hole injection efficiency could be realized by the increase of the QW number in a specific active layer. To achieve the uniform carrier distribution, structure C with increased five-pair $In_{0.11}Ga_{0.89}N$ QWs in the active layer I is proposed. The p-doped barriers and the active layer II in structure C are the same as in structure B.

The optical and physical properties of the GaN-based dual-wavelength LEDs are investigated numerically with the advanced physical models of semiconductor devices (APSYS) simulation program[26]. The light-extraction efficiency is assumed to be 0.78 in order to compare the simulation results with the experimental data[27]. The band-offset ratio is assumed to be 0.7/0.3 for both InGaN and AlGaN[28]. Note that the surface charges could be screened due to the defects inside the device, and that the amount obtained from the experimental measurement is usually smaller than that obtained by theoretical calculation with the self-consistent model[29,30]. In this letter, we assume the screen loss is 60%, and we take 40% of the calculated surface charges to match the experimental results[31]. The temperature is assumed to be 300 K in the simulation. The material parameters can be found in Ref. [32]. The other simulation parameters are the same as Ref. [33].

Figure 2 shows the electron and hole concentration around the active region of LEDs in three different structures at 60-mA current injection. As Fig. 2(a) shows, the hole concentration distribution in conventional LEDs is very non-uniform, the average hole concentration of $In_{0.18}Ga_{0.82}N$ QWs is two orders of magnitudes larger than that of the $In_{0.11}Ga_{0.89}N$ QWs. In the InGaN QWs, the high-In-component well has smaller width of forbidden band than the low-In-component one. As a result, the depth of QW with high-In component is deeper and the energy barrier for holes is lower, leading to the non-uniform distribution of hole concentration in QWs between the high- and low-In components. However, as shown in Fig. 2(b), by using the p-type barriers in structure B can promote the hole injection in $In_{0.11}Ga_{0.89}N$ QWs. The hole concentration in the low-In component well is enhanced markedly, and the non-uniform situation can be mitigated to a certain degree. Moreover, the hole concentrations in four QWs of the LED become quite uniform in structure C by using p-type barriers and specific number of the $In_{0.11}Ga_{0.89}N$ QWs, as shown in Fig. 2(c). Note that the electron concentration shows a slight decrease in the last several QWs near the p-side due to the use of gradually increased p-doped barriers in structures B and C. Clearly, the distribution of electrons and the holes in active region can be improved effectively by using the new designs.

Figure 3 shows the vertical (material growth direction) electron current density profiles around the active region with current injections of 60, 120, 240, 360, and 450 mA. The electrons are injected into the active region from the n-side and recombine with holes in the QWs, which results in the decrease of electron current density (mark with grey bars in Fig. 3). The electron current that escapes from the active region and then overflows from the p-side is viewed as the electron leakage current. Strong electrostatic fields appear in the active region of GaN-based LEDs due to the spontaneous and piezoelectric polarization, and the conduction band on the n-side

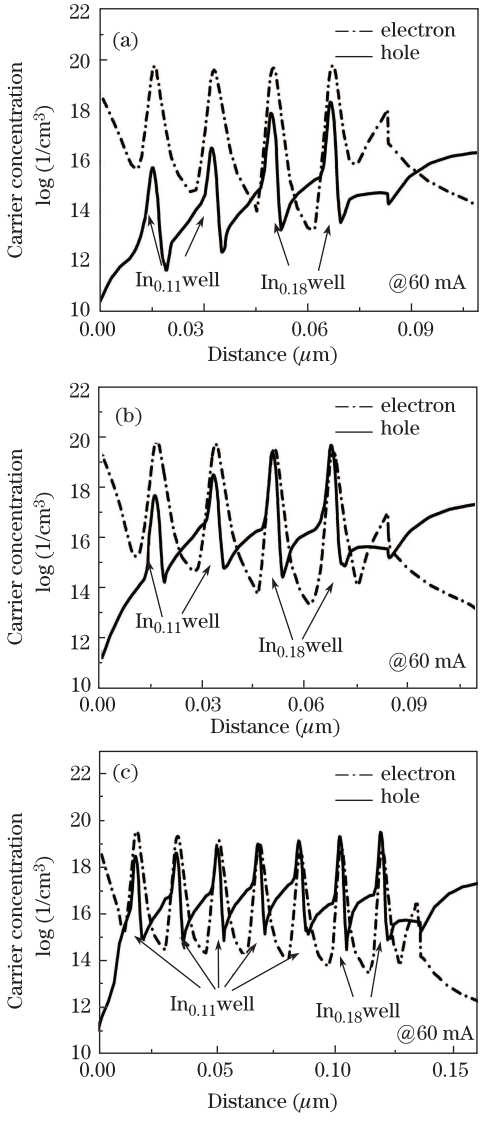

Fig. 2. Carrier concentrations of (a) conventional structure, (b) structure B, and (c) structure C around the active region at 60 mA.

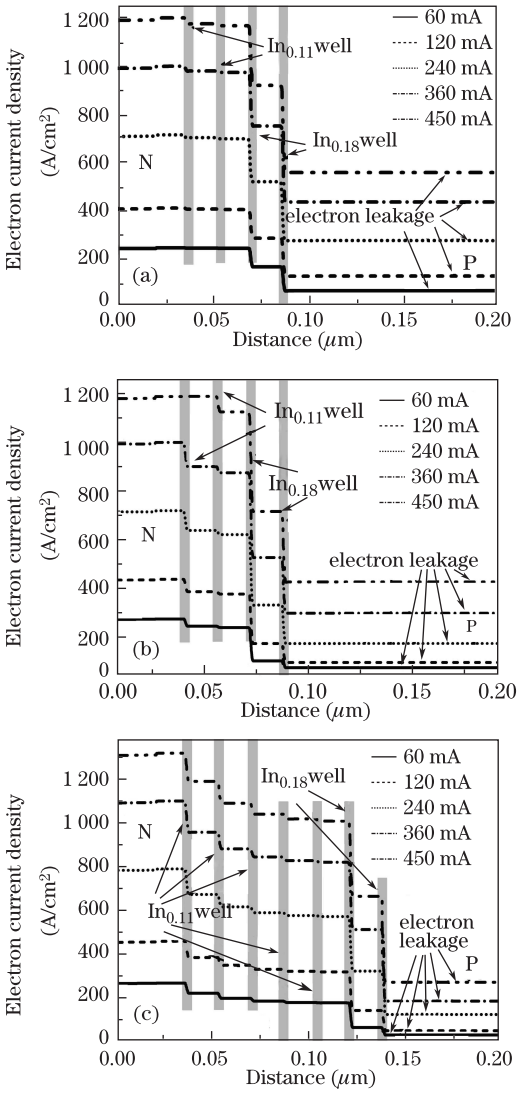

Fig. 3. Vertical electron current density profiles around the active region of (a) conventional structure, (b) structure B, and (c) structure C at different current injections.

becomes even higher than that of p-side. This severe band-bending will make a large number of electrons spill over from the p-side. As shown in Fig. 3, the electron leakage current can be observed in all three structures. In conventional structure, as shown in Fig. 3(a), the electron leakage current is severe and becomes even worse with the increase of current injection. As a result, the recombination of carriers is nearly absent in the $In_{0.11}Ga_{0.89}N$ QWs. On the contrary, Fig. 3(b) shows that, in structure B more carriers can participate in recombination and the electron leakage current is decreased, thereby showing the effectiveness of using p-doped barriers in QWs. Figure 3(c) shows that the lowest electron leakage current is achieved in structure C by using the p-doped barriers and with increase number of five-pair vertically stacked QWs in the active layer I. Moreover, the electron leakage current (265 A/cm^2) of structure C is significantly less than that of the conventional structure (551 A/cm^2) and structure B (404 A/cm^2) at the large current injection of 450 mA. These results mean that structure C has a better performance in the condition of large current injection. The reason is obvious: due to the much less electron spill over from the p-side, more carriers can be confined in the QWs, and the recombination of carriers is more frequent.

Figure 4 shows the spectra of the LEDs at 60, 120, 240, 360, and 450-mA current injections. As shown in Fig. 4(a), the spectrum intensity of the $In_{0.18}Ga_{0.82}N$ QWs (460 nm) is much higher than that of the $In_{0.11}Ga_{0.89}N$ QWs (410 nm) due to the stronger confinement for holes in high-In-component QWs than the low-In-component ones. In addition, with the increase of the current injection, the enhancement of curve peak for $In_{0.18}Ga_{0.82}N$ QW is much greater than that of the $In_{0.11}Ga_{0.89}N$ QWs. The dual-wavelength spectrum is quite non-uniform, and the situation worsens when the current injection is increased. The two peaks in the spectrum of structure B remain non-uniform, as shown in Fig. 4(b); however, the spectrum intensity is much larger than that of conventional structure, and the enhancement of curve peak for the $In_{0.11}Ga_{0.89}N$ QWs becomes more obvious

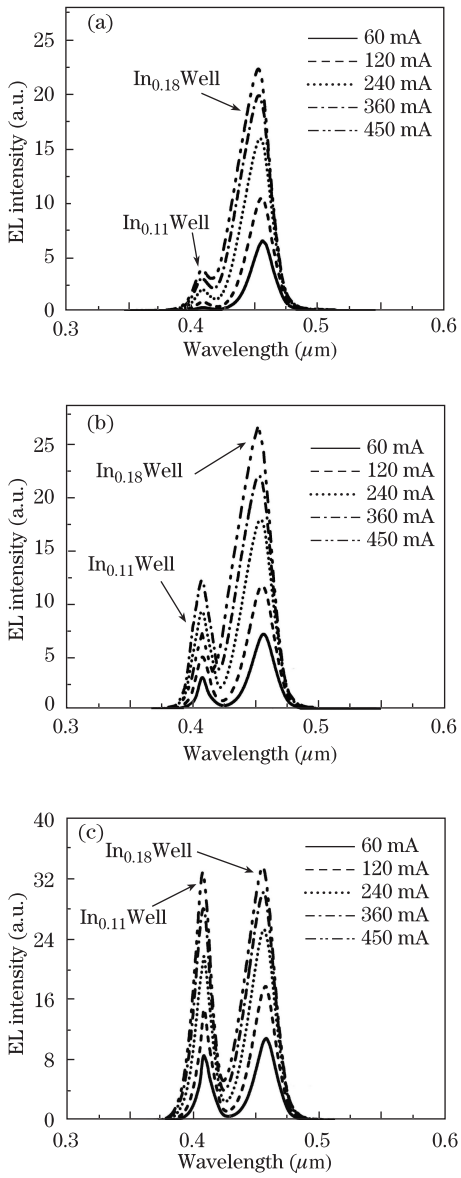

Fig. 4. Spectra of (a) conventional structure, (b) structure B, and (c) structure C at different current injections.

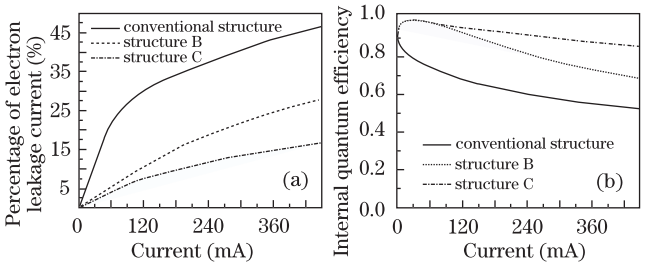

Fig. 5. (a) Percentage of electron leakage current and (b) IQE of conventional structure, structure B, and structure C at different current injections.

with the increase of current injection. These results show that the non-uniform situation is mitigated compared with the conventional LEDs. structure C has the best optical performance among the three structures, as shown in Fig. 4(c); the curve peaks of dual-wavelength tend to be quite uniform with the increase of current injection, and the spectrum intensity appears to be the strongest in the three structures. These results indicate that better optical performance of LED could be realized by promoting the equilibrium of carrier distribution and decreasing the electron leakage current.

Figure 5(a) illustrates the percentage of electron leakage current overflow from the active region versus the increase of current injection. It shows that the conventional structure has the largest percentage of electron leakage current, which reaches nearly 50% at 450-mA current injection. This result means that nearly half of the current injected into the active layer will spill over from the p-side of the LED under the condition of large current injection. However, the situation improves when p-type doped QW barriers are adopted in structure B; a smaller percentage of electron leakage current is achieved compared with the conventional structure. Structure C has the smallest percentage of leakage currents among the three structures. The leak percentage in structure C is merely 16.7%, even at the large current injection of 450 mA. Figure 5(b) shows the internal quantum efficiency (IQE) versus the increase of current injection. As shown in Fig. 5(b), IQE shows a drop tendency with the increase of the current injection in all three structures. However, the conventional structure has the worst IQE behavior due to the large electron leakage current and the poor hole injection efficiency, with the efficiency droop reaching 41.5% at 450-mA current injection. IQE is enhanced remarkably in structures B and C with p-doped QW barriers. Specifically, the efficiency droop decreases to 13.7% at 450 mA in structure C with p-doped QW barriers and increased the number of vertically stacked QWs.

In conclusion, the optical performance of dual-wavelength LEDs is enhanced with p-doped barriers and specific number of vertically stacked QWs. Higher IQE, stronger spectrum intensity, lower efficiency droop, and uniform peaks in the emission spectrum can be achieved using the new design of structure C. Through the simulation of physical properties with carrier distribution and electron current density, the above improvements in the new design of LED are found to be due to the better confinement of the electrons and the promotion of hole injection efficiency in the active region.

This work was supported by the National Natural Science Foundation of China (No. 61176043), the Fund for Strategic and Emerging Industries of Guangdong Province (No. 2010A081002005), and the Project of Combination of Production and Research by Guangdong Province and Ministry of Education of China (No. 2010B090400192).

References

1. M. C. Schmidt, K. C. Kim, H. Sato, N. Fellows, H. Masui, S. Nakamura, S. P. DenBaars, and J. S. Speck, Jpn. J. Appl. Phys. **46,** L126 (2007).
2. I. Ozden, E. Makarona, A. V. Nurmikko, T. Takeuchi, and M. Krames, Appl. Phys. Lett. **79,** 2532 (2001).
3. Y. Y. Zhang and G. H. Fan, Chin. Phys. B **20,** 048502 (2011).
4. B. Damilano, N. Grandjean, C. Pernot, and J. Massies, Jpn. J. Appl. Phys. **40,** L918 (2001).
5. M. Yamada, Y. Narukawa, and T. Mukai, Jpn. J. Appl. Phys. **41,** L246 (2002).
6. K. Akita, T. Kyono, Y. Yoshizumi, H. Kitabayashi, and K. Katayama, J. Appl. Phys. **101,** 033104 (2007).
7. M. F. Schubert, J. Xu, J. K. Kim, E. F. Schubert, M. H. Kim, S. Yoon, S. M. Lee, C. Sone, T. Sakong, and Y. Park, Appl. Phys. Lett. **93,** 041102 (2008).
8. Y. L. Li, T. Gessmann, E. F. Schubert, and J. K. Sheu, J. Appl. Phys. **94,** 2167 (2003).
9. I. A. Pope, P. M. Smowton, P. Blood, J. D. Thomson, M. J. Kappers, and C. J. Humphreys, Appl. Phys. Lett. **82,** 2755 (2003).
10. N. Tansu and L. J. Mawst, Appl. Phys. Lett. **82,** 1500 (2003).
11. N. Tansu and L. J. Mawst, J. Appl. Phys. **97,** 054502 (2005).
12. W. W. Chow, M. H. Crawford, J. Y. Tsao, and M. Kneissl, Appl. Phys. Lett. **97,** 121105 (2010).
13. J. Hader, J. V. Moloney, and S. W. Koch, Appl. Phys. Lett. **99,** 181127 (2011).
14. H. Zhao, G. Liu, J. Zhang, J. D. Poplawsky, V. Dierolf, and N. Tansu, Opt. Express **19,** A991 (2011).
15. H. Zhao, G. Liu, and N. Tansu, Appl. Phys. Lett. **97,** 131114 (2010).
16. C. T. Liao, M. C. Tsai, B. T. Liou, S. H. Yen, and Y. K. Kuo, J. Appl. Phys. **108,** 063107 (2010).
17. S. H. Park, D. Ahn, J. Park, and Y. T. Lee, Jpn. J. Appl. Phys. **50,** 072101 (2011).
18. J. Zhang, H. Zhao, and N. Tansu, Appl. Phys. Lett. **98,** 171111 (2011).
19. S. Choi, H. J. Kim, S. S. Kim, J. P. Liu, J. Kim, J. H. Ryou, R. D. Dupuis, A. M. Fischer, and F. A. Ponce, Appl. Phys. Lett. **96,** 221105 (2010).
20. L. Zhang, K. Ding, N. X. Liu, T. B. Wei, X. L. Ji, P. Ma, J. C. Yan, J. X. Wang, Y. P. Zeng, and J. M. Li, Appl. Phys. Lett. **98,** 101110 (2011).
21. H. Zhao, G. Liu, R. A. Arif, and N. Tansu, Solid-State Electronics **54,** 1119 (2010).
22. W. Lee, M. H. Kim, D. Zhu, A. N. Noemaun, J. K. Kim, and E. F. Schubert, J. Appl. Phys. **107,** 063102 (2010).
23. P. M. Tu, C. Y. Chang, S. C. Huang, C. H. Chiu, J. R. Chang, W. T. Chang, D. S. Wuu, H. W. Zan, C. C. Lin, H. C. Kuo, and C. P. Hsu, Appl. Phys. Lett. **98,** 211107 (2011).
24. M. C. Tsai, S. H. Yen, and Y. K. Kuo, Appl. Phys. Lett.

98, 111114 (2011).
25. Y. K. Kuo, S. H. Horng, S. H. Yen, M. C. Tsai, and M. F. Huang, Appl. Phys. A **98,** 509 (2010).
26. APSYS by Crosslight Software Inc., Burnaby, Canada (http://www.crosslight.com).
27. Y. K. Kuo, J. Y. Chang, M. C. Tsai, and S. H. Yen, Appl. Phys. Lett. **95,** 011116 (2009).
28. J. Piprek and S. Nakamura, IEE J. Optoelectron. **149,** 145 (2002).
29. H. Zhao, R. A. Arif, and N. Tansu, J. Appl. Phys. **104,** 043104 (2008).
30. J. Zhang, H. Zhao, and N. Tansu, Appl. Phys. Lett. **97,** 111105 (2010).
31. Y. K. Kuo, J. Y. Chang, and M. C. Tsai, Opt. Lett. **35,** 3285 (2010).
32. I. Vurgaftman and J. R. Meyer, J. Appl. Phys. **94,** 3675 (2003).
33. Y. K. Kuo, T. H. Wang, J. Y. Chang, and M. C. Tsai, Appl. Phys. Lett. **99,** 091107 (2011).